Oxidation of 2-Propanol by Peroxo Titanium Complexes: A Combined Experimental and Theoretical Study

Daniel H. Friese,[§] Christof Hättig,*[,§] Markus Rohe,[||] Klaus Merz,[†] André Rittermeier,[⊥] and Martin Muhler[‡]

Lehrstuhl für Anorganische Chemie I, Ruhr-Universität Bochum, Universitätsstraβe 150, D-44801 Bochum, Germany, Lehrstuhl für Technische Chemie, Ruhr-Universität Bochum, Universitätsstraβe 150, D-44801 Bochum, Germany, and Lehrstuhl für Theoretische Chemie, Ruhr-Universität Bochum, Universitätsstraβe 150, D-44801 Bochum, Germany

Received: July 24, 2010; Revised Manuscript Received: September 23, 2010

The oxidation of 2-propanol by titanium peroxo complexes is investigated in a combined synthetic, spectroscopic, and computational study. We find in quantum chemical calculations for the thermal reaction in protic solvents that the temporary protonation of the peroxo group activates the latter as electrophile. This transient species is amenable to a concerted transfer of two electrons and a proton from the secondary C atom of 2-propanol. Simultaneously, the carbonyl group is formed and the alcoholic proton is transferred to the solvent. In line with the results of the calculations, we find experimentally that the activity of the titanium peroxo complexes as oxidant depends on the pH value of the reaction medium.

1. Introduction

The oxidation of organic substrates in the presence of titanium dioxide is currently an intensive research area.[1−5] On a molecular basis, however, little is known about the processes that take place on the surface of solid titanium dioxide. In the case of the thermal and photochemical oxidation of 2-propanol, several products are reported.[6−8]

During both thermal and photochemical alcohol oxidation processes, active species are generated at the TiO_2 surface. Molecular adsorbed oxygen and reduced oxygen species have been observed by using temperature-programmed desorption (TPD) and oxidation (TPO) methods.[9,10] Once formed, these active species either react back to reforming alcohol, or dehydrogenate, or dehydrate to form products like propene, acetone, mesityloxide, and carbon dioxide.[11] In particular, the thermal process forms propene in remarkable amounts.[6,10] To investigate the role of reduced oxygen in the thermal oxidation of 2-propanol, we transform the situation from the catalyst surface to a molecular level. By following a model catalyst approach, we synthesized well-defined titanium-oxo complexes modified by peroxo units and additional metal ions.

Peroxo-rich metal-oxo complexes are suitable substances to achieve deeper insight in the mechanism of the oxidation processes. Furia et al.[12,13] investigated the thermal oxidation of secondary alcohols in the presence of vanadium and molybdenum peroxo complexes. On the basis of kinetic experiments, a radical pathway was postulated where the oxidation of the alcohol occurs coordinated to the metal center.

We have previously reported that different metal-containing titanium peroxo complexes show high activity in the photooxidation of 2-propanol, whereas similar complexes without any peroxo units did not show any activity in the photochemical oxidation.[14−16] In this work, we present a combined experimental and theoretical study on the thermal oxidation of 2-propanol by well-defined peroxo-rich molecular TiO complexes. The thermal oxidation of 2-propanol was monitored by in situ IR measurements, and the reaction mechanism was studied by quantum chemical calculations. As a suitable molecular model, we used water-soluble peroxo titanium complexes, which are accessible by hydrolysis of $TiCl_4$ in the presence of H_2O_2, NH_3, and citric acid or nitrilotriacetic acid. The incorporation of metal centers in these complexes can be achieved by treatment with appropriate metal salts.

2. Experimental Section

2.1. Preparation of $K_2[Ti(O_2)N(CH_2COO)_3]_2O \times 5\ H_2O$. Titanium(IV)chloride (2.2 mL, 20 mmol) was added dropwise to 30 mL of distilled water cooled in an ice bath. During hydrolysis, 20 mL (0.65 mol) of hydrogen peroxide (30%) and 3.8 g (20 mmol) nitrilotriacetic acid were added. Afterwards the pH value was adjusted to 2 by addition of 6 M aqueous solution of potassium hydroxide. The desired product crystallizes at 4 °C after several days from a water/THF mixture in the form of yellow-orange needles. The yield was 14.2 g (88.9%) for $K_2[Ti(O_2)N(CH_2COO)_3]_2O \times 5\ H_2O$.

$Li_2(NH_4)_4[Ti_2(O_2)_2(cit)(Hcit)]_2 \times 5\ H_2O$ and $(NH_4)_2[Ti(O_2)N(CH_2COO)_3]_2O \times 4\ H_2O$ were prepared using the literature procedures.[14,17]

2.2. IR Spectroscopy. ATR spectra were recorded using a heated HATR flow cell for ARK (Thermo) equipped with a ZnSe internal reflection element (IRE, 80 × 10 × 5 mm). The cell was mounted in a Nicolet Nexus FTIR spectrometer equipped with a mercury−cadmium-telluride (MCT-A) detector. Spectra were acquired at 4 cm^{-1} resolution accumulating 300 scans. The liquids were placed in a homemade glass reactor and were continuously circulated through the cell with a gear pump (ISMATEC Reglo-ZS). All flow rates used in the

* To whom correspondence should be addressed: Tel: +49 234 32 28082, Fax: +49 234 32 14045, E-mail: christof.haettig@theochem.rub.de.
† Lehrstuhl für Anorganische Chemie I, Ruhr-Universität Bochum.
‡ Lehrstuhl für Technische Chemie, Ruhr-Universität Bochum.
§ Lehrstuhl für Theoretische Chemie, Ruhr-Universität Bochum.
|| Present address: Sachtleben Chemie GmbH, LAB, Dr.-Rudolf-Sachtleben-Str. 4, 47198 Duisburg, Germany.
⊥ Present address: Bayer Technology Services GmbH, BTS-PT-RPT-REC, Leverkusen, E 41, Germany.

10.1021/jp1069175 © 2010 American Chemical Society
Published on Web 10/22/2010

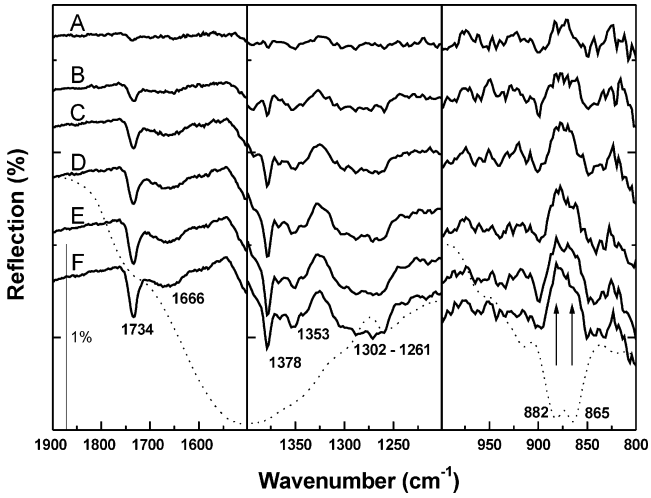


Figure 1. In situ ATR difference spectra of the oxidation of 3.2 mol % 2-propanol in hexadecane at 373 K after A) 60 min, B) 120 min, C) 180 min, D) 240 min, E) 300 min, F) 360 min. The dotted line shows an ATR spectrum of the cluster-coated IRE (reference: empty ATR cell). The reference was recorded 30 min after addition of 2-propanol to hexadecane at 373 K.

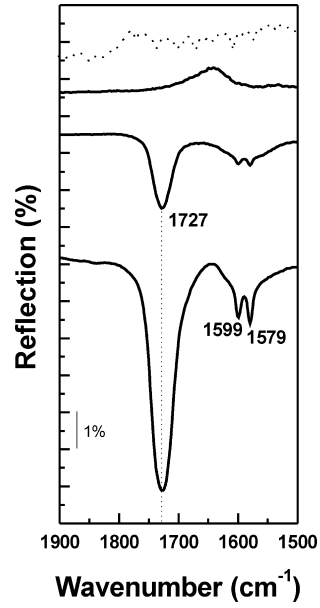


Figure 2. In situ ATR difference spectra of the oxidation of 2-propanol A) at 353 K, B) at 373 K after 5 min, C) at 373 K after 10 min. The dotted line shows an ATR spectrum of 2-propanol (reference: empty ATR cell). The reference spectrum is 2-propanol at 353 K.

experiments were 5 mL/min. Reference spectra were recorded, while the glass reactor was flushed with argon.

2.3. Thin Film Preparation. A solution of the cluster was prepared from about 5 mg cluster and 5 mL water. The solution was dropped onto the ZnSe IRE. After evaporation of the solvent in air, loose particles were removed by a nitrogen flow.

3. Computational Methods

The structures of educts, products, intermediates, and transition states of the studied reactions were determined by full geometry optimizations using DFT with the B3-LYP functional[18] and triple-ζ valence basis sets TZVP.[19] For all stationary points, it was checked that they are equilibrium or transition structures by calculating the vibrational frequencies and the energy differences reported in the following include the zero-point vibrational corrections obtained at the DFT/B3-LYP/TZVP level. To obtain a measure for the remaining correlation error of the B3-LYP functional, we performed in addition at the B3-LYP/TZVP geometries single point calculations with the recently devised double hybrid functional B2-PLYP,[20] which includes a perturbative second-order correlation part. The B3-LYP and B2-PLYP results are for all reaction and activation energies similar. Typically the results obtained with the two functionals agree within 10 kJ/mol. We report therefore in the following, if not stated otherwise, only the B3-LYP results. The B2-PLYP energies are available in the Supporting Information to this article. All calculations were carried out with the *TURBOMOLE V5.10* program package.[21]

4. Results

Figure 1 shows the oxidation of 2-propanol (3,2 mol % in hexadecane) over the cluster-coated IRE at 373 K. The bands at 882 and 865 cm^{-1} in the dotted spectrum belong to the ν(O−O) vibration of the peroxo group in the cluster. During the reaction, a consecutive reduction of the intensity of these bands is observed, which points to the consumption of the peroxo group. The bands at 1378 and 1353 cm^{-1} can be assigned to the $\delta_s(CH_3)$ vibrations of 2-propanol and acetone respectively and the broad interfering bands from 1302−1261 cm^{-1} to the δ(OH) vibration of 2-propanol and the citrate group of the cluster. They indicate a strong interaction of 2-propanol with the cluster.[22,23] The band at 1734 cm^{-1} originates from the ν(CO) vibration of acetone.[6,24,25] A very small broad band at 1666 cm^{-1} appears, which corresponds to the δ(OH) vibration of H_2O.[23] In Figure 2, the oxidation of pure 2-propanol on the coated IRE is shown. Only at this high concentration of the educt small additional new bands at 1599 and 1579 cm^{-1} are observed (Figure 2), which indicate the presence of carbon double bonds of mesityl oxide. The formation of carbon dioxide and propene was not observed under the chosen reaction conditions.[6]

The Raman spectra of the remaining solid after the oxidation show the total degradation of the peroxo units (not shown). To study the reaction mechanism and selectivity of the oxidation process, in situ GC-MS measurements were carried out. The analyses of the spectra indicate acetone as main product and mesityl oxide and propene as side products.

This observation corresponds to work of Xu[6,7] who studied the production of propene in the thermal oxidation of 2-propanol on titania surfaces. In contrast to the thermal dehydration of 2-propanol, we have shown that the photochemical oxidation of 2-propanol exclusively leads to the formation of acetone and CO_2.[14]

Comparable studies of the thermal oxidation of 2-propanol in the liquid phase using peroxo nitrilotriacetic complexes $(NH_4)_2[Ti_2(O_2)_2N(CH_2COO)_3O]$ and $K_2[Ti_2(O_2)_2N(CH_2COO)_3O] \times 5\ H_2O$ show in contrast to the potassium complex an enhanced activity in the case of the ammonium complex.

For the peroxo titanium cluster with the nitrilotriacetate (NTA) ligands $(NH_4)_2[Ti_2(O_2)_2(N(CH_2COO)_3)_2O]$, we studied the reaction mechanism of the thermal oxidation of 2-propanol by means of quantum chemical calculations with the DFT approach as described in section 3. Initially, the titanium peroxo cluster and the alcohol form a hydrogen bonded complex with the ammonium counterions. Because of the presence of several carboxylate groups, ammonium cations and the alcohol OH group this complex has a large flexibility to arrange in various geometries conserving the strong O···HO, O···HN, and N···HO hydrogen bonds. It can in particular arrange to a tautomeric form with a protonated peroxo group, where the

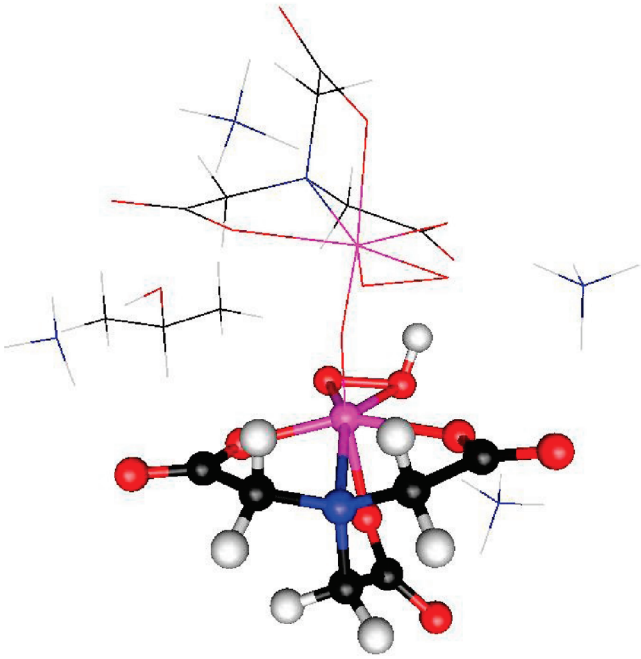


Figure 3. Structure of the transient tautomer that is formed before the transition state is reached. The protonation of the peroxo group facilitates the approach of the H−C group.

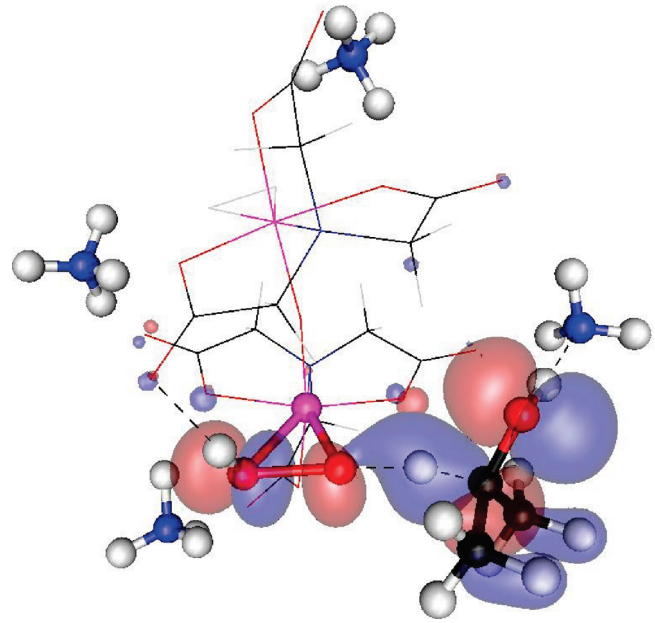


Figure 4. Interaction between the O−O antibonding orbital of the peroxo group with the HOMO of 2-propanol at the transition state structure. The HOMO of 2-propanol is at this structure an antibonding combination of the H−C σ bond and the lone pair of the O atom in the alcohol. Transfer of the respective electron pair to the peroxo group thus leads to a simultaneous breaking of the H−C and O−O bonds together with the formation of the OH and C═O bonds.

resulting ammonia molecule is stabilized by a hydrogen bond to the OH group of the alcohol (Figure 3). This transient species is about 58 kJ/mol (calculated with B3-LYP/TZVP) higher in energy than the energetically more favorable tautomer with four ammonium cations. The protonation activates the peroxo group and makes it amenable for the transfer of a hydride ion from the alcohol, whereas ammonia acts as an acceptor for the proton of the alcohol group. The dehydrogenation of 2-propanol can thus take place in a concerted two-electron step, which leads directly to acetone and $[Ti_2(OH)_2(O_2)(N(CH_2COO)_3)_2O]^{3-}$ or $[Ti_2(OH_2)(OH)(O_2)(N(CH_2COO)_3)_2O]^{2-}$ (depending on the precise arrangement of the ammonium cations in the calculations). Calculated with respect to the transient species with the protonated peroxo group, we find an activation energy of 89 kJ/mol for the dehydrogenation (see Figure 4 for the transition state and the involved orbitals). With B2-PLYP/TZVP we obtain for the activation energy 79 kJ/mol, which gives an impression of the remaining uncertainty of the DFT calculations. Relative to the more favorable tautomer of the $(NH_4)_2[Ti_2(O_2)_2(N(CH_2COO)_3)_2O]\cdot HOCH(CH_3)_2$ complex, the total activation energy is 148 kJ/mol. For the reaction energy from $(NH_4)_2[Ti_2(O_2)_2(N(CH_2COO)_3)_2O]\cdot HOC(CH_3)_2$ to $(NH_4)_4Ti_2(OH)_2(O_2)(N(CH_2COO)_3)_2O]\cdot OC(CH_3)_2$, we obtained −221 kJ/mol. The initial reaction product $[Ti_2(OH)_2(O_2)(N(CH_2COO)_3)_2O]^{2-}$ can in a subsequent step eliminate water to form a Ti═O group. The B3-LYP/TZVP calculations predict the energy for this elimination step in the gas phase to be close to 0 kJ/mol, whereas the B2-PLYP/TZVP result of −13 kJ/mol indicates that the reaction already in the gas phase is slightly exothermic. In the liquid phase the evaporation enthalpy of water (44 kJ/mol at 298 K) has to be included in the theoretical results, which leads to total reaction energies of approximately −44 kJ/mol, so that $[Ti_2O(O_2)(N(CH_2COO)_3)_2O]^{2-}$ would be the energetically favored species. To investigate in more detail the role of the protic solvent in the activation of the peroxo group, we repeated the calculations with the ammonium cations replaced by potassium, which has a similar ionic radius but cannot act as proton donor. For these computations, we used a smaller $[Ti(O_2)(N(CH_2COO)_3)OCH_3]^-$ cluster where one $Ti(O_2)(N(CH_2COO)_3)$ fragment is replaced by a methyl group. For the smaller cluster model, we also performed calculations with ammonium counterions to compare the results directly.

In this smaller model with ammonium counterions, the results for the formation of the intermediate with the protonated peroxo group are similar to the ones in the larger model, although the activation barrier is found to be by 40 kJ/mol lower than for the larger system. Concerning the transition state structure, both models are very similar and it has to be taken into account that the interaction of the cluster with the mobile counterions has a large influence on the energy of the calculated structures. In solution, all free coordination sites would be saturated, which is not possible in our gas-phase model.

When we replace the ammonium counterions in this model by the similar-sized potassium cations, we find a significantly higher activation energy: It increases by almost 60 to 157 kJ/mol. The ammonium ions thus play an important role as proton donors and acceptors in the reaction mechanism.

5. Discussion

Raman spectra of similar complexes, which reacted under photochemical conditions,[15] show the significant degradation of the peroxo units in the reaction of 2-propanol with $Li_2(NH_4)_4[Ti_2(O_2)_2(cit)(Hcit)]_2 \times 5\ H_2O$ and the in situ IR experiments give information about the oxidation process of the secondary alcohol. The analyses of the IR spectra indicate the formation of adsorbed 2-propanol as potential intermediate of the oxidation process. Interestingly, besides the formation of the bands of the main product acetone, there are weak bands that indicate the formation of mesityl oxide as additionally formed side product. It is well-known that the oxidation process depends on several parameters and dehydrogenation contributes more for primary alcohols in comparison to secondary alcohols.[26,27] This is in

agreement with the additional DFT calculations on the reactivity of the peroxo unit and the formation of the main product acetone.

The mechanism for the thermal oxidation of 2-propanol to acetone by the peroxo titanium complex through a concerted transfer of a hydride ion and a proton resembles the mechanism for the oxidation with chromic acid and other transition metal oxidants[28] in the sense that it also involves a two-electron transfer. Unlike as in the oxidation with chromate, we do not find an initial coordination of the alcohol to the central metal atom but only coordination through hydrogen bridges to the ligands and the solvent shell of the peroxo titanium cluster. This coordination and a protonation of the peroxo group in an acidic solution facilitates the formation of an activated complex, where the H−C σ bond of the secondary alcohol can readily interact with the antibonding orbital of the peroxo group. This permits a simultaneous transfer of H^- to the peroxo group and the H^+ of the alcohol group to a solvent molecule. The important role of a protic solvent for an initial activation of the peroxo group is clearly shown by the large increase of the activation energy in the DFT calculations when the ammonium counterions are replaced by K^+. The results are comparable with the DFT calculations of Schneider,[29] who investigated the oxidation of thioether in the presence of peroxo-rich vanadium complexes. The protonation at the side-on peroxo unit is energetically favored and is necessary for the following oxidation step. This is in line with the experimental observation that the activity of peroxo titanium complexes in 2-propanol oxidation increases, when the potassium cation is replaced by the ammonium cation.

6. Conclusions

The combined in situ IR and theoretical investigation of the thermal oxidation of 2-propanol in the presence of peroxo-rich titanium complexes as molecular model of a TiO_2 surface with adsorbed reduced oxygen species provides deeper insight into the oxidation phenomena on the TiO_2 surface during the thermal oxidation process of 2-propanol. The calculations show that the first step of the oxidation process of the secondary alcohol is a protonation of the peroxo unit followed by a transfer of hydride ion from the C-2 atom of the alcohol to the peroxo group. The oxidation process was monitored by in situ IR measurements, which indicate the degradation of the peroxo units and the formation of the oxidation products.

Acknowledgment. We gratefully acknowledge financial support of the Deutsche Forschungsgemeinschaft (SFB 558 "Metall-Substrat-Wechselwirkungen in der heterogenen Katalyse").

Supporting Information Available: Equilibrium structures and energies from the electronic structure calculations at the DFT/B3LYP and DFT/B2PLYP level and the spectroscopic characterization data for $K_4[Ti(O_2)N(CH_2COO)_3]_2O \times 5\ H_2O$. This material is available free of charge via the Internet at http://pubs.acs.org.

References and Notes

(1) Thiruvenkatachari, R.; Vignenswaran, S.; Moon, I. S. *Korean J. Chem. Eng.* **2008**, *25*, 64.
(2) Tachikawa, T.; Fujitsuka, M.; Majima, T. *J. Phys. Chem. C* **2007**, *111*, 5259.
(3) Chen, J.; Ollis, D. F.; Rulkens, W. H.; Bruning, H. *Water Res.* **1998**, *33*, 669.
(4) Linsebigler, A. L.; Lu, G.; Yates, J. T., Jr. *Chem. Rev.* **1995**, *95*, 735.
(5) Nishida, Y.; Omichi, T.; Katayama, I.; Yamashita, H.; Narisawa, M.; Matsamura, Y. *e-J. Surf. Sci. Nanotech.* **2005**, *3*, 311.
(6) Xu, W.; Raftery, D.; Francisco, J. S. *J. Phys. Chem. B* **2003**, *107*, 4537.
(7) Xu, W.; Raftery, D. *J. Phys. Chem. B* **2001**, *105*, 4343.
(8) Arsac, F.; Bianchi, D.; Chovelon, J. M.; Ferronato, F.; Herrmann, J. M. *J. Phys. Chem. A* **2006**, *110*, 4213.
(9) Brinkley, D.; Engel, T. *J. Phys. Chem. B* **2000**, *104*, 9836.
(10) Brinkley, D.; Engel, T. *Surf. Sci.* **1998**, *415*, 1001.
(11) Bondarchuk, O.; Kim, Y. K.; White, J. M.; Kim, J.; Kay, B. D.; Dohnalek, Z. *J. Phys. Chem. C* **2007**, *111*, 11059.
(12) Campestrini, S.; Di Furia, F. *Tetrahedron* **1994**, *50*, 5119.
(13) Campestrini, S.; Di Furia, F.; Modena, G.; Novello, F. *Stud. Surf. Sci. Catal.* **1991**, *66*, 375.
(14) Rohe, M.; Merz, K. *Chem. Commun.* **2008**, *7*, 862.
(15) Rohe, M.; Merz, K. *Eur. J. Inorg. Chem.* **2008**, *2*, 3264.
(16) Rohe, M.; Löffler, E.; Muhler, M.; Birkner, A.; Wöll, C.; Merz, K. *Dalton Trans.* **2008**, 6106.
(17) Schwarzenbach, G.; Muehlebach, J.; Mueller, K. *Inorg. Chem.* **1970**, *9*, 2381.
(18) Becke, A. D. *J. Chem. Phys.* **1993**, *98*, 5648.
(19) Schäfer, A.; Huber, C.; Ahlrichs, R. *J. Chem. Phys.* **1994**, *100*, 5829–5835.
(20) Grimme, S. *J. Chem. Phys.* **2006**, *124*, 034108.
(21) *TURBOMOLE*; University of Karlsruhe and Forschungszentrum Karlsruhe GmbH, 1989−2007; available from http://www.turbomole.com.
(22) Arsac, F.; Bianchi, D.; Chovelon, J. M.; Ferronato, C.; Herrmann, J. M. *J. Phys. Chem. A* **2006**, *110*, 4202–4212.
(23) Rossi, P. F.; Busca, G.; Lorenzelli, V.; Saur, O.; Lavalley, J.-C. *Langmuir* **1987**, *3*, 52–58.
(24) El-Maazawi, M.; Finken, A. N.; Nair, A. B.; Grassian, V. H. *J. Catal.* **2000**, *191*, 138–146.
(25) Bürgi, T.; Bieri, M. *J. Phys. Chem. B* **2004**, *108*, 13364–13369.
(26) Kim, K. S.; Barteau, M. A. *J. Mol. Catal.* **1990**, *63*, 103.
(27) Farfan-Arribas, E.; Madix, R. J. *J. Phys. Chem. B* **2002**, *106*, 10680.
(28) Wiberg, K. B.; Schäfer, H. *J. Am. Chem. Soc.* **1969**, *91:4*, 933.
(29) Schneider, C. J.; Penner-Hahn, J. E.; Pecoraro, V. L. *J. Am. Chem. Soc.* **2008**, *130*, 2712.

JP1069175